Mon. Not. R. Astron. Soc. **297,** 108–116 (1998)

Scintillation parameters for 49 pulsars

Simon Johnston,[1] Luciano Nicastro[2] and Bärbel Koribalski[3]

[1]*Research Centre for Theoretical Astrophysics, University of Sydney, NSW 2006, Australia*
[2]*Instituto TeSRE – CNR, Via Gobetti 101, 40129 Bologna, Italy*
[3]*Australia Telescope National Facility, CSIRO, PO Box 76, Epping, NSW 2121, Australia*

Accepted 1998 January 5. Received 1997 October 10

ABSTRACT

We report on multi-epoch, multifrequency observations of 64 pulsars with high spectral and time resolution. Scintillation parameters were obtained for 49 pulsars, including 13 millisecond pulsars. Scintillation speeds were derived for all 49, which doubles the number of pulsars with speeds measured in this way. There is excellent agreement between the scintillation speed and proper motion for the millisecond pulsars in our sample using the simple assumption of a mid-placed scattering screen. This indicates that the scaleheight of scattering electrons is similar to that of the dispersing electrons. In addition, we present observations of the Vela pulsar at 14 and 23 GHz, and show that the scintillation bandwidth scales as $\nu^{3.93}$ over a factor of 100 in observing frequency. We show that for PSR J0742 − 2822, and perhaps PSR J0837 − 4135, the Gum nebula is responsible for the high level of turbulence along their lines of sight, contrary to previous indications. There is a significant correlation between the scintillation speeds and the product of the pulsar's period and period derivative for the 'normal' pulsars. However, we believe this to be caused by selection effects both in pulsar detection experiments and in the choice of pulsars used in scintillation studies.

Key words: pulsars: general – pulsars: individual: Vela – radio continuum: stars.

1 INTRODUCTION

Radio pulsars are high-velocity stars, with measured velocities of up to 1500 km s^{-1}. These velocities are thought to arise from asymmetric supernova explosions which impart a 'kick' to the newly born neutron star (Dewey & Cordes 1987). Evaluation of pulsar velocities yields $\sim$460 km s^{-1} as their mean velocity at birth (Lyne & Lorimer 1994). Millisecond pulsars have, in general, lower velocities than the 'normal' pulsars. Both Cordes & Chernoff (1997) and Lyne et al. (1998) find that the mean space velocity for millisecond pulsars lies between 120 and 160 km s^{-1}. Thus the millisecond pulsar velocities are drawn from the lower end of the 'normal' pulsar distribution, as only these pulsars are likely to remain bound to their binary companions after the supernova explosion (Tauris & Bailes 1996).

Three largely independent methods are available to measure a pulsar's velocity. The first is to measure the proper motion through timing observations over a period of many years. This method favours pulsars with low timing noise, expecially the millisecond pulsars (e.g. Lyne et al. 1998). The second is by using radio interferometry to obtain accurate measurements of the pulsar's position at different epochs. Such a technique has yielded proper motions for 86 pulsars (Bailes et al. 1990; Fomalont et al. 1992, 1997; Harrison, Lyne & Anderson 1993). This method is difficult and works best with high flux density pulsars, particularly those which also have strong extragalactic reference sources within a few degrees. The third technique involves measuring the interstellar scintillations (ISS) caused by electron density fluctuations along the line of sight to the pulsar. ISS velocities have been measured for about 70 pulsars (Cordes 1986; Nicastro & Johnston 1995).

Soon after the discovery of pulsars, it was realized that the measured fluctuations in the pulse intensity were not intrinsic to the source. The fluctuations can be described by a simple model consisting of a thin screen of scattering electrons located midway between the observer and the pulsar (Scheuer 1968). In general, the motion of the pulsar is different from, and much greater than, that of the screen. Thus, as the pulsar moves behind the screen, the radiation diffraction pattern sweeps past the observer, and this causes

the apparent change in the pulsar flux density. By measuring these changes, the velocity of the pulsar can be derived. Measurement of pulsar velocities through timing and interferometry techniques are generally limited to strong and/or nearby pulsars, unlike the ISS method which can probe both more distant and weaker objects. The disadvantages of ISS techniques are that the *vector* velocities cannot usually be measured and that systematic errors due to the velocity and placement of the scattering screen may be incurred.

Harrison et al. (1993) examined the correlation between ISS and interferometric velocities, and claimed that ISS velocities were, on average, lower than those obtained interferometrically. Harrison & Lyne (1993) then showed that scintillation velocities and interferometric velocities are similar for pulsars with low z-heights, but that the scintillation velocities are a factor of ~ 5 too low at z-heights of 1 kpc. They thus postulated that the scattering electrons had a scaleheight of only 50 pc, in contrast to the dispersing electrons which have a scaleheight of ~ 1 kpc (Reynolds 1989). This result was controversial, as it is widely believed that the same electrons were responsible for both dispersion and scattering.

Gupta (1995) revisited the discussion of the comparison of scintillation speeds and proper motion. Based on the Taylor & Cordes (1993) distance model and a revised formula for computing scintillation speeds (Gupta, Rickett & Lyne 1994), he showed that there was a good match between the two methods, independent of the z-height of the pulsar. Gupta (1995) gives the scintillation speed as

$$V_{\rm ISS} = A_V \frac{(D\Delta\nu_{\rm d}X)^{1/2}}{\nu t_{\rm d}}, \qquad (1)$$

where D is the distance to the pulsar in kpc, and ν is the observing frequency in GHz. The decorrelation time-scale, $t_{\rm d}$, is the time in seconds it takes for the pulsar's flux density to fall to 1/e, and the scintillation bandwidth, $\Delta\nu_{\rm d}$, is the bandwidth in MHz over which the pulsar's intensity falls to half its maximum. The constant A_V is derived by assuming a Kolmogorov turbulence spectrum and a homogeneously turbulent medium, and has been estimated as 3.85×10^4 (Gupta et al. 1994). X is the observer–screen distance divided by the pulsar–screen distance. Gupta (1995) found that an excellent fit could be obtained between the interferometric and scintillation speeds for $X - 1$, and thus found no need to introduce a low z-height screen.

2 OBSERVATIONS AND ANALYSIS

Observations of a sample of 64 southern pulsars were carried out at the 64-m Parkes radiotelescope. The observations were taken at eight different epochs between 1994 April and 1996 October. For the earlier observations, the centre frequency was 436 MHz. For the later observations, centre frequencies of 660 and 1520 MHz were used. Occasionally, observations were obtained at 4800 and 8400 MHz. Observations of the Vela pulsar at frequencies of 13.5 and 23 GHz were carried out in 1995 November. This project commenced in 1992 July; data taken prior to 1994 have been published in Nicastro & Johnston (1995) and Nicastro, Johnston & Koribalski (1996). In addition, scintillation parameters for the Be star binary pulsar PSR J1302 − 6350 (B1259 − 63) have been published elsewhere (McClure-Griffiths et al. 1998). For completeness, we include all results obtained to date.

Observations at frequencies below 1 GHz had a total bandwidth of 2×32 MHz subdivided into 256 filter channels, each of width 125 kHz. Observations at frequencies above 1 GHz used a filterbank with 64 channels, each of width 5 MHz. As the scintillation bandwidth roughly follows a ν^4 law, the spectral resolution at 1.5 GHz is well matched to that at 660 MHz, and many pulsars were observed at both frequencies. The filterbanks are sampled continuously at a fixed rate (between 0.3 and 1.2 ms, depending on the pulse period); the output from each channel is one-bit digitized and written to magnetic tape for off-line analysis. Individual observations were typically 30 min or longer.

During the analysis, we form pulse profiles at the apparent pulsar period over short sections in time and for each of the 256 (or 64) filter channels. These subintegration times were typically 10 to 60 s in duration. The signal-to-noise ratio in each subintregration for each frequency channel is then calculated. Malfunctioning channels, or channels with strong interference present, were usually overwritten by an average of the signal-to-noise ratio in adjacent channels. The dynamic spectra could then be summed along the frequency and time axes to improve the signal-to-noise ratio. Fig. 1 shows the dynamic spectrum for PSR J0452 − 1759 at 660 MHz with a resolution of 0.125 MHz in the frequency domain and 30 s in the time domain.

To obtain the scintillation bandwidth and decorrelation time-scale, we performed a two-dimensional autocorrelation analysis on the dynamic spectra, following the method described by Cordes (1986). An example of the autocovariance function produced for the dynamic spectrum shown in Fig. 1 is given in Fig. 2. The scintillation bandwidth, $\Delta\nu_{\rm d}$, and the decorrelation time-scale, $t_{\rm d}$, can then be obtained by fitting a Gaussian function to the zero lag in frequency and time respectively. Often, individual scintles do not remain at a fixed frequency, but 'drift' towards either higher or lower frequencies during the obvservation because of refractive scintillation effects (as can be seen in Fig. 2). The Gaussian fitting procedure takes these drifts into account when calculating the scintillation parameters.

3 RESULTS

Table 1 lists the 49 pulsars for which we were able to measure the scintillation bandwidth and time. Column 2 gives the pulsar identification (ID) to help distinguish the binary and/or millisecond pulsars. Pulsars without ID are single, 'normal' pulsars. Columns 3 to 5 give the spin periods, distances and z-heights of the pulsars. The distance to the pulsar is derived from its dispersion measure (DM) using the electron density model of Taylor & Cordes (1993), except where parallax or H I absorption measurements have been obtained. For these pulsars we include a reference number as superscript on the distance. In column 6 we give the centre frequency of the observations, followed in column 7 by the total integration time at that frequency. Columns 8 to 10 give the scintillation bandwidth, the decorrelation time and the scintillation speed according to equation (1). These quoted figures are the average of all observations of a particular pulsar. In the final column we

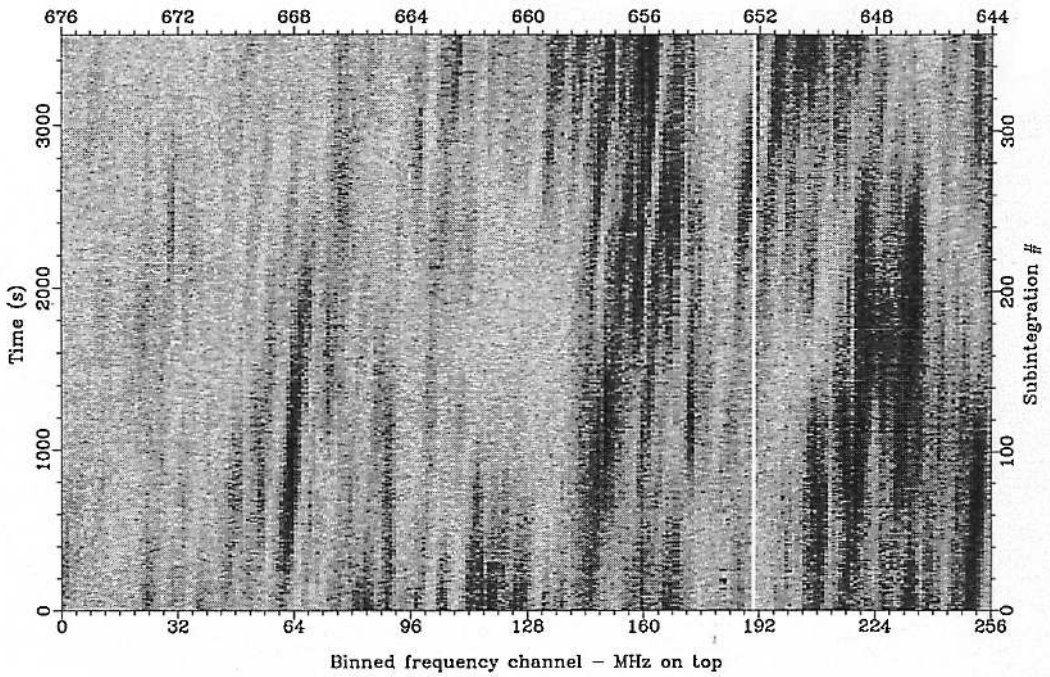

Figure 1. Dynamic spectrum of PSR J0452 − 1759 at 660 MHz with a frequency resolution of 0.125 MHz and a subintegration time of 30 s. The grey-scale shows signal strength, increasing from white to black.

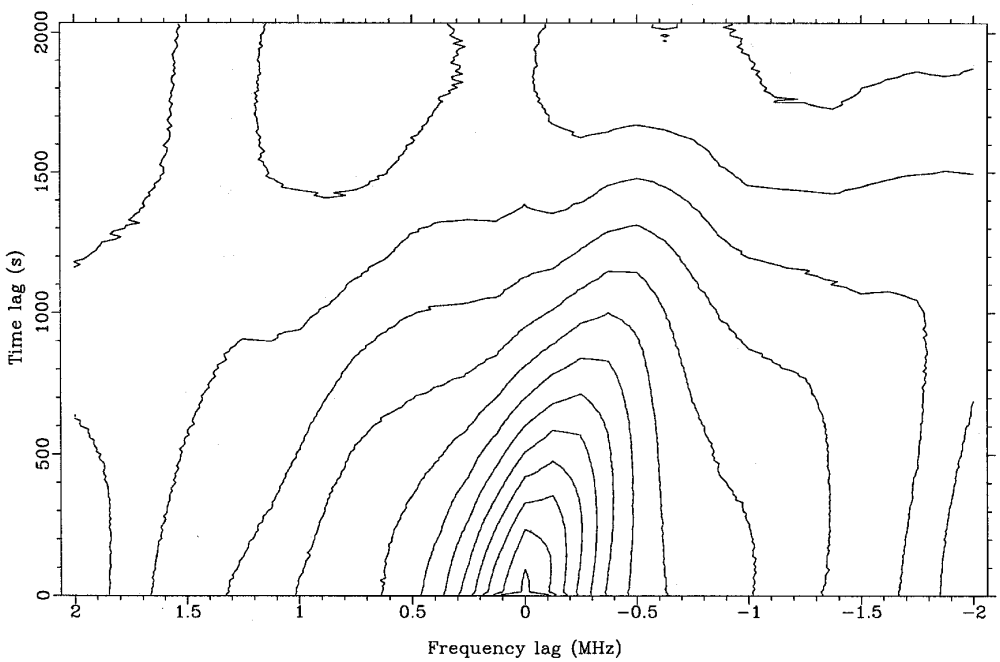

Figure 2. Contour plot of the autocorrelation coefficient for the dynamic spectrum shown in Fig. 1. Contour levels start at 0.8 (near the origin) and decrease in steps of 0.05.

give $\log(C_N^2)$, a measure of the average turbulence along the line of sight, which Cordes (1986) gives as

$$C_N^2 = 0.002\, \nu^{11/3} D^{-11/6} \Delta\nu_d^{-5/6}, \quad (2)$$

with ν in GHz, D in kpc and $\Delta\nu_d$ in MHz. The 'canonical' value of $\log(C_N^2)$ is -3.5 for typical lines of sight through the local ISM. Higher values than this represent higher than average levels of turbulence.

We failed to determine scintillation parameters for 15 pulsars from our original sample. This list includes three millisecond pulsars, PSRs J0034 − 0534, J1025 − 08 and J1804 − 2718, which are all too weak to observe with high spectral and/or time resolution. Other weak pulsars are PSRs J0459 − 0212, J1320 − 3512, J1358 − 2533, J1720 − 0212 and J1908 − 0734. There are six strong pulsars in the sample for which an adequate signal-to-noise ratio

Table 1. Scintillation parameters for 49 pulsars.

PSR J	ID	P (ms)	D (kpc)	z-height (kpc)	ν (MHz)	T (hr)	$<\Delta\nu_d>$ (MHz)	$<t_d>$ (s)	$<V_{ISS}>$ (km s^{-1})	$<\log C_N^2>$
0034−0721		942.95	0.68	−0.64	436	0.50	3.80	> 1800	< 40	−3.8
					660	5.00	7.55	> 3600		
0134−2937		136.96	1.78	−1.76	436	3.00	0.52	296	310	−4.2
					660	4.00	3.49	521		
					1388	2.50	33.5	625		
0255−5304		447.71	1.15	−1.08	1388	3.0	42.7	1910	100	−3.6
0401−7608		545.25	1.52	−0.89	436	1.50	0.22	362	200	−3.9
					660	3.50	2.95	575		
0437−4715	BM	5.76	0.18[a]	−0.12	436	15.45	3.61	470	170	−3.1
					660	1.0	17.4	600		
0452−1759		548.94	3.14	−1.76	660	3.50	0.50	828	110	−3.9
					1388	4.50	5.27	1170		
0536−7543		1245.85	1.05	−0.54	436	1.00	0.25	185	300	−3.6
					660	2.43	1.93	291		
					1388	1.00	24.8	479		
					1520	2.00	82.6	587		
0711−6830	SM	5.49	1.03	−0.41	436	8.22	0.37	800	81	−3.7
					660	3.00	1.16	931		
0742−2822		166.75	2.00[b]	−0.08	660	3.02	–	58	53	−1.5
					4800	2.23	8.83	638		
					8400	1.07	40.0	2260		
0835−4510		89.30	0.50	−0.02	4800	0.89	–	40	130	+0.5
					8400	1.08	13.9	70		
					13700	3.42	58.2	133		
					22400	1.00	–	260		
0908−4913		106.76	6.67	−0.12	1520	3.00	12.0	4770	48	−4.4
0942−5552		664.37	6.34	−0.25	660	2.50	0.19	251	290	−4.2
0953+0755		253.06	0.127[c]	0.09	436	0.67	2.00	1270	33	−2.6
1057−5226		197.11	1.53	0.18	660	4.17	2.52	276	440	−4.0
					1388	0.75	36.8	308		
1243−6423		388.48	12.2	−0.33	4800	0.42	4.9	221	280	−2.8
1302−6350	BV	47.76	1.50[d]	−0.03	4800	33.34	8.5	190	150	−1.3
					8400	13.33	70.0	360		
1418−3921		1096.78	5.04	1.75	660	0.50	0.25	406	160	−4.1
1430−6623		785.44	1.80	−0.17	660	2.57	0.28	93	450	−3.4
1453−6413		179.48	2.70[b]	−0.21	660	2.33	0.15	95	400	−3.5
1455−3330	BM	7.99	0.73	0.28	436	8.27	1.37	1060	81	−3.9
1456−6843		263.38	0.45[e]	−0.07	436	2.43	1.40	1800	49	−3.4
					660	0.50	2.80	973		
1537+1155	BV	37.90	0.68	0.51	436	6.23	1.53	681	190	−3.8
1544−5308		178.55	1.29	0.03	1520	1.50	6.80	155	490	−2.9
1559−4438		257.06	2.00[b]	0.22	660	2.50	0.16	77	400	−3.2
1603−7202	BM	14.84	1.64	−0.42	660	0.50	0.36	553	81	−3.4
1605−5257		658.01	1.24	−0.01	1520	1.50	20.2	731	170	−3.3
1614+0737		1206.80	1.50	0.93	436	0.50	0.16	34	880	−3.5
					1520	0.50	15.0	240		
1709−4428		102.45	2.80[b]	−0.13	436	1.50	<0.2	–	89	−4.2
					1520	2.5	32.1	2800		
1713+0747	BM	4.57	0.89	0.38	436	1.22	1.45	1700	29	−3.5
1730−2304	SM	8.12	0.50	0.05	436	6.38	0.17	564	62	−2.8
					660	1.00	1.34	583		
					1520	3.23	29.8	1620		
1744−1134	SM	4.07	0.17	0.03	436	3.30	1.34	1260	31	−2.5
					660	2.92	2.30	1190		
1751−4657		742.35	1.07	−0.19	436	1.00	0.25	147	180	−3.1
					660	3.67	0.23	354		
1807−0847		163.73	3.61	0.35	4800	1.13	8.35	484	91	−2.0
1825−0935		768.97	1.03	0.02	660	2.50	0.22	404	73	−2.8
1848−1952		4308.19	0.96	−0.14	436	0.50	0.23	112	230	−3.4
					1520	1.78	43.7	1000		
1911−1114	BM	3.62	1.58	−0.26	436	1.50	0.16	146	180	−3.7
1946+1805		440.62	0.85	−0.05	660	1.50	0.52	797	49	−3.0
1949−2524		957.61	1.32	−0.52	436	0.50	0.15	161	240	−3.7
					660	2.33	1.48	339		
2051−0827	BMV	4.50	1.26	−0.63	436	2.30	0.33	566	100	−3.8
2053−7200		341.33	0.94	−0.54	436	1.00	0.55	715	150	−3.8
					660	2.00	5.55	668		

Table 1 – *continued*

PSR J	ID	P (ms)	D (kpc)	z-height (kpc)	ν (MHz)	T (hr)	$<\Delta\nu_d>$ (MHz)	$<t_d>$ (s)	$<V_{ISS}>$ (km s^{-1})	$<\log C_N^2>$
2124−3358	SM	4.93	0.24	−0.17	436	3.67	6.90	2650	40	−3.5
2129−5718	BM	3.73	2.55	−1.76	436	0.75	0.29	636	130	−4.2
					660	1.57	1.25	1020		
					1520	1.53	58.0	1460		
2144−3933		2836.63	0.33	−0.25	436	1.25	0.32	559	48	−2.8
					660	1.00	2.90	1500		
2145−0750	BM	16.05	0.50	−0.34	436	8.12	1.48	1510	51	−3.6
2155−3118		1030.00	0.93	−0.72	436	1.17	0.60	366	160	−3.6
					660	2.48	1.77	486		
2317+1439	BM	3.44	1.89	−1.27	436	1.00	0.48	812	100	−4.3
2317+2149		1444.65	1.40	−0.82	436	0.50	0.40	578	110	−4.0
2330−2005		1643.62	0.49	−0.46	436	2.00	0.35	269	140	−2.9
					660	3.15	1.20	346		
					1388	1.50	24.0	1590		
2346−0610		1181.45	1.95	−1.75	660	3.50	1.22	335	350	−3.9
					1388	3.25	24.5	524		

S – Single pulsar, B – Binary pulsar, M – Millisecond pulsar, V – Variations with binary phase.
References: [a]Sandhu et al. (1997), [b]Koribalski et al. (1995), [c]Gwinn et al. (1986), [d]McClure-Griffiths et al. (1998), [e]Bailes et al. (1990).

could be obtained in narrow spectral channels and short time integrations. These are PSRs J0738 − 4042, J0837 − 4135, J1001 − 5507, J1604 − 4909, J1731 − 4744 and J1900 − 2600. These pulsars are relatively distant and probably have scintillation bandwidths much less than 0.125 kHz at 660 MHz. Finally, we believe that the scintillation time-scale for PSR J0108 − 1431 is extremely long, and that the scintillation bandwidth is also larger than the total bandwidth available, as expected for a pulsar with the smallest known DM. As far as we are aware, there are no published scintillation parameters for any of these pulsars apart from PSR J0837 − 4135, for which Johnston et al. (1996) derived a scintillation bandwidth of 310 kHz and a decorrelation time-scale of 350 s at 1.4 GHz, and PSR J0738 − 4042, for which Ramachandran et al. (1997) quote a value of 76 ms for the scattering time (equivalent to a scintillation bandwidth of 2 Hz) at 327 MHz. These figures for the scintillation bandwidth are significantly below our spectral resolution.

4 DISCUSSION

Fig. 3 shows a plot of $\log(C_N^2)$ versus distance for the 49 pulsars in our sample. As is evident, the bulk of the pulsars have $D \lesssim 3$ kpc and have values of $\log(C_N^2)$ scattered about the 'expected' value of −3.5. Four pulsars have $\log(C_N^2) \gtrsim -2.0$. PSRs J0835 − 4510 and J0742 − 2822 are located behind the Gum nebula, and are discussed in more detail below. PSR J1302 − 6350 is located just behind an enhanced density region within a spiral arm (McClure-Griffiths et al. 1998). PSR J1243 − 6423 is unlikely to be as distant as the Taylor & Cordes (1993) model suggests. It probably also lies behind an high-density region of the same spiral arm as PSR J1302 − 6350. The high value of PSR J1807 − 0847 is probably due to its location within 12° of the Galactic Centre.

Surprisingly, three of the four pulsars in our sample with $D \gtrsim 5$ kpc (including the non-detections listed above) have $\log(C_N^2) \lesssim -4.0$. PSRs J0908 − 4913 and J0942 − 5552 are

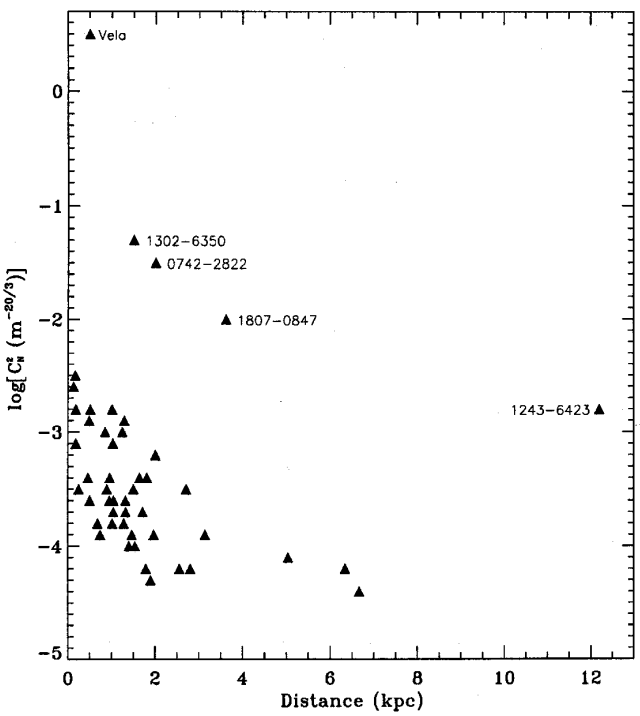

Figure 3. $\log(C_N^2)$ against distance for the 49 pulsars in our sample.

both low-latitude pulsars, whereas PSR J1418 − 3921 is at a high galactic latitude, and its distance of 5 kpc is a lower limit in the Taylor & Cordes (1993) model. Either these lines of sight suffer from low levels of turbulence throughout their path-length, or the distance to the pulsar may be overestimated by a factor of 2–3. It is also possible that the individual scintiles are not well resolved by our hardware; all three values of scintillation bandwidth are close to the resolution limit. A much smaller scintillation bandwidth would result in a larger value of $\log(C_N^2)$.

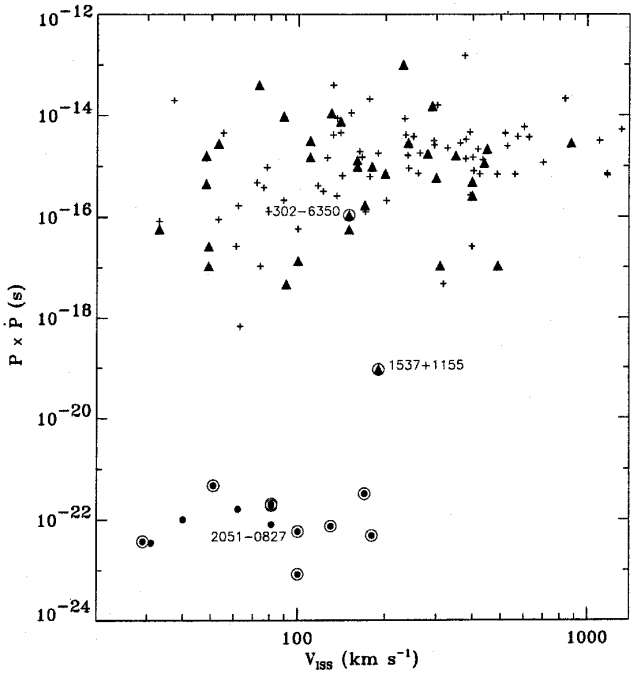

Figure 4. The product of the pulsar period and period derivative against the scintillation velocity. Triangle symbols denote 'normal' pulsars from this work, and plus symbols are from Cordes (1986). All millisecond pulsars are denoted by filled circles, and all binary pulsars are marked with an additional ring. Binary pulsars whose parameters change as a function of orbital phase are marked.

Fig. 4 shows the scintillation velocity as a function of the product of the pulsar period and period derivative ($P\dot{P}$; equivalent to the square of the magnetic field). In this figure we have included all the pulsars from our sample and those from the sample of Cordes (1986). For the latter sample, we have updated the scintillation velocities using new distance estimates and equation (1) (see Gupta 1995). In Fig. 4 the two classes of pulsar can easily be distinguished. The millisecond pulsars (bottom left of the figure) have velocities less than 200 km s^{-1}. The two intermediate spin-period pulsars in the group, PSRs J1302−6350 and J1537+1155, have relatively high velocities; however, both these are undoubtedly over-esimtates as, in the first case, the scattering screen is located close to the pulsar and, in the second, the orbital velocity dominates the measured value.

Cordes (1986) found that the scintillation speed and $P\dot{P}$ were significantly correlated for the non-millisecond pulsars, although there is no apparent physical explanation why this should be the case. The Spearman rank-order correlation coefficient, using the non-millisecond pulsars from the combined samples, is 0.24 and is significant at the 98 per cent confidence level. However, the correlation is significantly different between our sample and that of Cordes (1986). His sample yields a correlation coefficient of 0.32, significant at greater than the 99 per cent confidence level, whereas our sample has a correlation coefficient of less than 0.05. The reasons for this are unclear. One possibility is that our sample is largely restricted to nearby pulsars because of our lack of spectral resolution. This biases our sample towards low-velocity pulsars in the solar neighbourhood. We also have a number of (older) pulsars in our sample which are above the scattering layer. For these pulsars, the scintillation velocity is an underestimate of the true value and hence restricts their range of velocities. Finally, we have not included our 12 non-detections in our statistical analysis. As discussed above, at least six of these are likely to have high velocities, and only one a low velocity. This bias must again affect the correlation coefficient. Thus we believe that whatever mild correlation there appears to be in the data is almost certainly caused by hard-to-quantify selection effects of one type or another. For example, it is difficult to discover high-velocity, old pulsars because such pulsars will typically be at high z-heights and hence have low flux densities. This could account for the lack of pulsars in the diagram with $P\dot{P} \sim 10^{-16}$ and speeds $\gtrsim 200$ km s^{-1}, and possibly create the observed correlation. In sum, there is no clear-cut consensus on the significance (if any) of the velocity–magnetic field correlation (Lorimer, Lyne & Anderson 1995).

Only six pulsars in our sample have scintillation speeds $\gtrsim 400$ km s^{-1}, with PSR J1614+0737 being the highest measured at 880 km s^{-1}. Of the non-millisecond pulsars, nine have velocities less than 100 km s^{-1}. The large number of slow-moving pulsars is probably not indicative of the underlying population. Two important effects play a role in our sample. First, we choose relatively nearby pulsars so that their decorrelation bandwidth is larger than our spectral resolution. Old, nearby pulsars are likely to be rather slow-moving. Secondly, pulsars above the scattering electron layer will have their scintillation speeds underestimated using equation (1) with $X = 1$.

4.1 Millisecond pulsars

We have measured scintillation speeds for 13 millisecond pulsars, four of which are single, and nine of which are binary pulsars with white dwarf companions. Given the small sample, it is difficult to draw conclusions about any difference in the velocity distribution between the single and binary pulsars. However, we note that two of the four single pulsars have velocities less than 50 km s^{-1}, and that none has a velocity in excess of 100 km s^{-1}. Of the nine binary pulsars, five have velocities greater than 100 km s^{-1}.

Significant proper motions have been obtained for nine of these millisecond pulsars, and this sample can be used to test the correlation between the scintillation speeds and the timing velocities. The pulsars are all well within the (dispersing) electron layer, and one might expect $X \sim 1$ and the Harrison & Lyne (1993) correction factor to have only a small effect. The scintillation speeds agree with the proper motion within the errors for five of these: PSRs J1455−3330, J1713+0747, J1730−2304, J1744−1134 and J2145−0750. Of the remaining four PSRs J0437−4715 and J2317+1439 have a marginally higher scintillation speed than proper motion velocity, whereas for PSRs J0711−6830 and J2124−3358 the reverse is true. The average ratio of the proper motions to the scintillation speed for this sample of nine pulsars is 1.05. Thus the derivation of the scintillation speeds by Gupta (1995) provides an excellent fit to the data. If we apply the Harrison & Lyne (1993) formula to the data, the derived scintillation speeds

are consistently too small. This is reflected in the average ratio of 1.78 between the proper motion and scintillation speeds.

Upper limits to the pulsar's velocity can be obtained from knowledge of the pulsar's period derivative using the so-called Shklovskii effect (Shklovskii 1970; Camilo, Thorsett & Kulkarni 1994). For three of the four pulsars without a measured proper motion, PSRs J1603 − 7205, J1911 − 1114 and J2129 − 5718, this limit is 120, 235 and 350 km s^{-1} respectively. The scintillation speeds are all less than these upper limits. Finally, PSR J2051 − 0827 has a low proper motion, only 25 km s^{-1} (Stappers 1997). The scintillation velocity appears higher than this, but for this pulsar, the scintillation parameters vary significantly with orbital phase (see also Stappers et al. 1996). It is likely that the wind blown from the companion star is contributing to the scintillation parameters. A more complete investigation of the scintillation parameters of this pulsar is underway.

PSR J1911 − 1114 has the highest scintillation speed of any millisecond pulsar in our sample at 180 km s^{-1}. PSR J2129 − 5718 is the most distant millisecond pulsar in the sample. The Taylor & Cordes (1993) model gives only a lower distance limit of 2.6 kpc to the pulsar. The scintillation velocity of 135 km s^{-1} is already high, and this can be considered a lower limit, as the scattering screen is presumably closer to the Earth than to the pulsar in this case.

4.2 Individual pulsars

PSR J0034 − 0721: The decorrelation time-scale for this pulsar, even at 660 MHz is remarkably long, in escess of 1 h, similar to the result of Cordes (1986). We can only set up upper limit to the pulsar's velocity of 40 km s^{-1}.

PSR J0134 − 2937: This pulsar has a galactic latitude of − 80°. The Taylor & Cordes (1993) distance model assigns it only a lower distance limit of 1.8 kpc. Its scintillation speed of 310 km s^{-1} is likely to be an underestimate of its true speed, due to the unknown distance of the pulsar and the fact that the screen responsible for the scattering is likely to be closer to the observer than the pulsar. The pulsar has a short spin-period (140 ms) and a low period derivative, and thus lies to the right of the spin-up line in the period–period derivative plane. This pulsar is likely to have been mildly recycled by a companion star and has become a runaway following the second supernova explosion in the system.

PSR J0452 − 1759: According to the Taylor & Cordes (1993) distance model this pulsar is beyond the dispersion electron layer, and the model indicated a lower distance limit of 3.1 kpc. At this distance the proper motion yielded a velocity of 580 ± 200 km s^{-1} (Fomalont et al. 1992), which has since been revised to 320 ± 200 km s^{-1} (Formalont et al. 1997). The uncertainties preclude a definite statement, but the proper motion appears to be higher than the scintillation velocity of 110 km s^{-1}. This is another case where we know that the scattering screen is significantly closer to the Earth than to the pulsar, as the dispersion electrons (in the Taylor & Cordes model) extend out to only ∼1 kpc. Having such a close screen biases the scintillation velocities towards lower values. We note that both the scintillation bandwidth and the decorrelation time for this pulsar are significantly larger than that given in Cordes (1986).

PSR J0536 − 7543: We have measurements of the scintillation bandwidth of this pulsar at 436, 660 and 1520 MHz. Between 436 and 1520 MHz, the frequency dependence is 4.6 ± 0.25, and between 660 and 1520 MHz it is 4.5 ± 0.6. This is consistent with the expected frequency dependence for a Kolmogorov turbulence spectrum of 4.4.

PSR J0742 − 2822: The DM-derived distance of the pulsar is 1.9 kpc. H I absorption measurements towards this pulsar give a lower distance limit of 2.0 kpc and an upper limit of 6.7 kpc (Koribalski et al. 1995). At a distance of 2 kpc, the proper motion of the pulsar (Bailes et al. 1990; Fomalont et al. 1997) implies a transverse velocity of 260 km s^{-1}. The scintillation velocity is only 53 km s^{-1}. The turbulence along this line of sight, as measured by $\log(C_N^2)$ is very high at − 1.5, higher than for most other pulsars, though significantly less than for Vela. Data on this pulsar taken at 1.33 GHz (D. Stinebring, private communication) show a scintillation time-scale of ∼190 s and a decorrelation bandwidth of ∼50 kHz. The derived velocity of 48 km s^{-1} confirms our higher frequency observations.

In order to reconcile the scintillation velocity with the proper motion, the screen must be significantly closer to Earth than to the pulsar. We thus surmise that the Gum nebula, located only a few hundred parsecs away, is responsible for the enhanced scattering in the direction of PSR J0742 − 2822. Although the Vela pulsar has long been known to suffer from enhanced scattering for its distance and location, this has generally been attributed to the surrounding SNR rather than to the Gum nebula. However, this may need to be revised in the light of the results of PSR J0742 − 2822. Further evidence for the Gum nebula as a significant source of scattering may come from PSR J0837 − 4135. Its scintillation velocity is only 30 km s^{-1} (Johnston et al. 1996) and, although its proper motion is not known, this low velocity is significantly less than the proposed mean velocity for pulsars at birth. Again, a nearby scattering screen could be the cause.

PSR J0835 − 4510: The Vela pulsar has been extensively observed at frequencies below 5 GHz; scintillation parameters are given in Roberts & Ables (1982). Here, for the first time, we present scintillation parameters for Vela at 8.4, 13.7 and 22.4 GHz. The proper motion of the Vela pulsar is 140 km s^{-1} (Bailes et al. 1989) if we assume a distance of 500 pc. Using the measurements of both scintillation bandwidth and decorrelation time at 8.4 and 13.7 GHz, we obtain a scintillation speed of 130 km s^{-1}. This is similar to the proper motion and would imply that the scattering screen is located roughly halfway to the pulsar. This seems to be in contradiction to the VLBI results of Desai et al. (1992), who measure the angular broadening of Vela to claim that the scattering screen is located 80 per cent of the way to the pulsar. However, Britton (1996) has shown that these figures may be reconciled if one assumes that the scattering material is roughly comoving with the pulsar, i.e., in some sort of bow-shock.

There are now measurements of the scintillation bandwidth of the Vela pulsar from 160 MHz to 13.7 GHz. At the lowest frequencies the scintillation bandwidth can be obtained from the reciprocal of the duration of the scattering tail. Over a factor of ∼85 in observing frequency, the scintillation bandwidth increases by a factor of $\sim 5 \times 10^7$. Taking values of the scintillation bandwidth from the litera-

ture at 0.16, 0.25, 0.30, 1.42, 1.67, 3.2 and 5.0 GHz with observations obtained here, we find that the scintillation bandwidth follows a $\nu^{3.93}$ law throughout this frequency range. As previously noted, this is inconsistent with a Kolmogorov turbulence spectrum, but is consistent with scattering from discrete sources, presumably either within the Gum nebula and/or the Vela supernova remnant. If this law continues to hold to higher frequencies, then the Vela pulsar should remain in the strong scintillation regime until $\sim$80 GHz. The decorrelation time-scale has now been measured from 1.4 GHz up to 22.4 GHz, and shows the expected $\nu^{6/5}$ relationship.

PSR J0953 + 0755: The scintillation bandwidth of this pulsar differs significantly throughout the literature. Our value of 2.0 MHz at an observing frequency of 436 MHz is consistent with the results of Cordes, Weisberg & Boriakoff (1985) and Cordes (1986). However, it is significantly smaller than other values or lower limits quoted elsewhere (Rickett 1970; Armstrong & Rickett 1981; Roberts & Ables 1982; Phillips & Clegg 1992). In particular, Phillips & Clegg (1992), observing a 50 MHz, find the bandwidth to be 30 kHz, which implies that the pulasr would not be in strong scattering at frequencies above 400 MHz. Their inferred $\log(C_N^2)$ of -4.7 is the lowest known of any pulsar, which they attribute to the line of sight being mainly through the local bubble.

If all the results are taken at face value, it thus appears as if PSR J0953 + 0755 has wildly varying scintillation bandwidths over time-scales of a few years. Variations in scintillation bandwidth of factors of a few are certainly more common in closer pulsars, but variations such as these are unprecedented in any other pulsar. Further and more frequent observations of this pulsar at low frequencies are necessary to solve this puzzle.

PSR J1430 − 6623: The proper motion gives a velocity of 320 km s^{-1} for this pulsar (Bailes et al. 1990). The scintillation velocity is higher at 450 km s^{-1}. In this case it is possible that our scintillation bandwidth is slightly over-estimated because of a lack of spectral resolution.

PSR J1453 − 6413: H I observations have shown that this pulsar is further away than the DM distance would suggest (Koribalski et al. 1995). Adopting a distance of 2.7 kpc, the scintillation speed of 400 km s^{-1} is somewhat higher than the proper motion of 335 km s^{-1} (Bailes et al. 1990).

PSR J1456 − 6843: This is a nearby pulsar with a parallax distance of 450 pc and a proper motion of 88 km s^{-1} (Bailes et al. 1990). The scintillation velocity is somewhat lower at 40 km s^{-1}.

PSR J1559 − 4438: The pulsar has been assigned its lower distance limit of 2 kpc from H I observations (Koribalski et al. 1995). The proper motion of Fomalont et al. (1992) is non-significant for this pulsar. The scintillation velocity is 400 km s^{-1}.

PSR J1709 − 4429: We have commented on this pulsar in a separate paper (Nicastro, Johnston & Koribalski 1996), and we ruled out the proposed association of the pulsar with the supernova remnant G 343.1 − 2.3 (McAdam, Osborne & Parkinson 1993). Even with the revised scintillation formula for Gupta (1995), the velocity of 89 km s^{-1} is insufficient for it to have originated at the centre of the SNR.

PSR J1730 − 2304: Observations of the pulsar at both 436 and 1520 MHz imply a frequency dependence of the scintillation bandwidth of 4.14 ± 0.25.

PSR J1807 − 0847: The proper motion is not significant for this pulsar; the 1σ upper limit is 155 km s^{-1} (Fomalont et al. 1997). The scattering strength of the pulsar as measured by $\log(C_N^2)$ is two orders of magnitude greater than the norm, perhaps due to its location only 12° from the Galactic Centre. It has a scintillation velocity of only 91 km s^{-1}. Although our decorrelation time is consistent with the extrapolation from 1 GHz (Cordes 1986), the scintillation bandwidth is substantially less than that expected from a ν^4 law. It is not possible to tell from the Cordes (1986) paper at which frequency this pulsar was observed; at low frequencies the individual scintles would not have been well resolved.

PSR J1825 − 0935: Fomalont et al. (1997) give a value of 75 ± 45 km s^{-1} for the proper motion of this pulsar. This is consistent with our scintillation velocity of 73 km s^{-1}. The measured scintillation bandwidth and decorrelation time-scale are consistent with the results of Cordes (1986). However, the results of Gil et al. (1994), who quote a decorrelation time-scale of 150 min, are clearly in error.

PSR J2330 − 2005: We have measurements of the scintillation bandwidth of this pulsar at 436, 660 and 1388 MHz. Between 436 and 1388 MHz, the frequency dependence is 3.7 ± 0.3, and between 660 and 1388 MHz it is 4.0 ± 0.5. These values are somewhat lower than the expected value of 4.4 for a Kolmogorov turbulence spectrum.

PSR J2346 − 0610: This pulsar is above the electron layer, and only a lower limit on the distance can be obtained. The scintillation velocity of 350 km s^{-1} can probably be considered as a lower limit, as the scattering screen is likely to be closer to the observer than to the pulsar.

5 CONCLUSIONS

In the first comprehensive survey of scintillation parameters from the southern hemisphere, we have measured the scintillation speeds of 49 pulsars. When combined with a similar survey from the northern hemisphere (Cordes 1986), more than 100 pulsars now have speeds measured in this way.

Of our sample, 13 are millisecond pulsars. Prior to this work, only three other millisecond pulsars had measured scintillation parameters. There is some indication that the single millisecond pulsars have a smaller velocity than the binary pulsars. A comparison between the scintillation speeds and the proper motion of nine millisecond pulsars shows that the Gupta (1995) derivation of the scintillation speeds provides a much better fit to the data than that of Harrison & Lyne (1993). Like Gupta (1995), we thus see no need to postulate that the electrons responsible for the scattering are different to those responsible for the dispersion measure.

For the first time we present scintillation observations of the Vela pulsar at frequencies up to 23 GHz. We show that the scintillation bandwidth follows a ν^4 power law, and that the decorrelation time follows a $\nu^{6/5}$ law over nearly a factor of 100 in observing frequency.

PSR J0742 − 2822 has the third largest C_N^2 of the pulsars in the sample after the Vela pulsar and PSR J1302 − 6350. We surmise that the high level of turbulence along this line

of sight is caused by a filament or other high-density structure associated with the Gum nebula. Surprisingly, three rather distant pulsars have values of $\log(C_N^2)$ less than -4.

For the 'normal' pulsars in our sample, there is no correlation between the scintillation speeds and the product of the pulsar's period and period derivative. This is contrary to the result found by Cordes (1986). In the combined sample, there does appear to be a significant correlation, but we argue this is likely to be due to selection effects.

ACKNOWLEDGMENTS

Hardware used in this work was designed and built by A. Lyne at Jodrell Bank, University of Manchester. We thank Y. Gupta for many useful discussions during the course of this work. The Parkes radio telescope is part of the Australia Telescope, which is funded by the Commonwealth of Australia for operation as a National Facility managed by CSIRO.

REFERENCES

Armstron J. W., Rickett B. J., 1981, MNRAS, 194, 623
Bailes M., Manchester R. N., Kesteven M. J., Norris R. P., Reynolds J. E., 1989, ApJ, 343, L53
Bailes M., Manchester R. N., Kesteven M. J., Norris R. P., Reynolds J. E., 1990, MNRAS, 247, 322
Britton M. C., 1996, PhD thesis, Univ. California, Santa Barbara
Camilo F., Thorsett S. E., Kulkarni S. R., 1994, ApJ, 421, L15
Cordes J. M., 1986, ApJ, 311, 183
Cordes J. M., Chernoff D. F., 1997, ApJ, 482, 971
Cordes J. M., Weisberg J. M., Boriakoff V., 1985, ApJ, 288, 221
Desai K. M. et al., 1992, ApJ, 393, L75
Dewey R. J., Cordes J. M., 1987, ApJ, 321, 780
Formalont E. G., Goss W. M., Lyne A. G., Manchester R. N., Justtanont K., 1992, MNRAS, 258, 497
Fomalont E. B., Goss W. M., Manchester R. N., Lyne A. G., 1997, MNRAS, 286, 81
Gil J. A. et al., 1994, A&A, 282, 45
Gupta Y., 1995, ApJ, 451, 717
Gupta Y., Rickett B. J., Lyne A. G., 1994, MNRAS, 269, 1035
Gwinn C. R., Taylor J. H., Weisberg J. M., Rawley L. A., 1986, AJ, 91, 338
Harrison P. A., Lyne A. G., 1993, MNRAS, 265, 778
Harrison P. A., Lyne A. G., Anderson B., 1993, MNRAS, 261, 113
Johnston S., Koribalski B. S., Weisberg J., Wilson W., 1996, MNRAS, 279, 661
Koribalski B. S., Johnston S., Weisberg J., Wilson W., 1995, ApJ, 441, 756
Lorimer D. R., Lyne A. G., Anderson B., 1995, MNRAS, 275, L16
Lyne A. G., Lorimer D. R., 1994, Nat, 369, 127
Lyne A. G. et al., 1998, MNRAS, in press
McAdam W. B., Osborne J. L., Parkinson M. L., 1993, Nat, 361, 516
McClure-Griffiths N., Johnston S., Stinebring D., Nicastro L., 1998, ApJ, 492, L49
Nicastro L., Johnston S., 1995, MNRAS, 273, 122
Nicastro L., Johnston S., Koribalski B., 1996, A&A, 306, 49
Phillips J. A., Clegg A. W., 1992, Nat, 360, 137
Ramachandran R., Mitra D., Deshpande A. A., McConnell D. M., Ables J. G., 1997, MNRAS, 290, 260
Reynolds R. J., 1989, ApJ, 339, L29
Rickett B. J., 1970, MNRAS, 150, 67
Roberts J. A., Ables J. G., 1982, MNRAS, 201, 1119
Sandhu J. S., Bailes M., Manchester R. N., Navarro J., Kulkarni S. R., Anderson S. B., 1997, ApJ, 478, L95
Scheuer P. A. G., 1968, Nat, 218, 920
Shklovskii I. S., 1970, AvA, 13, 562
Stappers B. W., 1997, PhD thesis, Australian National Univ.
Stappers B. W. et al., 1996, ApJ, 465, L119
Tauris T. M., Bailes M., 1996, A&A, 315, 432
Taylor J. H., Cordes J. M., 1993, ApJ, 411, 674